The Journal of Immunology

MicroRNA-146a Feedback Inhibits RIG-I-Dependent Type I IFN Production in Macrophages by Targeting TRAF6, IRAK1, and IRAK2

Jin Hou, Pin Wang, Li Lin, Xingguang Liu, Feng Ma, Huazhang An, Zhugang Wang and Xuetao Cao

---

Supplementary Material	http://www.jimmunol.org/content/suppl/2009/07/14/jimmunol.0900707.DC1
References	This article **cites 46 articles**, 12 of which you can access for free at: http://www.jimmunol.org/content/183/3/2150.full#ref-list-1

Why *The JI*? Submit online.

- **Rapid Reviews! 30 days*** from submission to initial decision

- **No Triage!** Every submission reviewed by practicing scientists

- **Fast Publication!** 4 weeks from acceptance to publication

*average

Subscription	Information about subscribing to *The Journal of Immunology* is online at: http://jimmunol.org/subscription
Permissions	Submit copyright permission requests at: http://www.aai.org/About/Publications/JI/copyright.html
Email Alerts	Receive free email-alerts when new articles cite this article. Sign up at: http://jimmunol.org/alerts

MicroRNA-146a Feedback Inhibits RIG-I-Dependent Type I IFN Production in Macrophages by Targeting TRAF6, IRAK1, and IRAK2[1]

Jin Hou,[2]*[†] Pin Wang,[2][†] Li Lin,[2][‡] Xingguang Liu,[†] Feng Ma,[‡] Huazhang An,[†] Zhugang Wang,[3][§] and Xuetao Cao[3]*[†][‡]

Upon recognition of viral components by pattern recognition receptors, including TLRs and retinoic acid-inducible gene I (RIG-I)-like helicases, cells are activated to produce type I IFN and proinflammatory cytokines. These pathways are tightly regulated by host to prevent inappropriate cellular response, but viruses can down-regulate these pathways for their survival. Recently, identification of negative regulators for cytoplasmic RNA-mediated antiviral signaling, especially the RIG-I pathway, attract much attention. However, there is no report about negative regulation of RIG-I antiviral pathway by microRNAs (miRNA) to date. We found that vesicular stomatitis virus (VSV) infection up-regulated miR-146a expression in mouse macrophages in TLR-myeloid differentiation factor 88-independent but RIG-I-NF-κB-dependent manner. In turn, miR-146a negatively regulated VSV-triggered type I IFN production, thus promoting VSV replication in macrophages. In addition to two known miR-146a targets, TRAF6 and IRAK1, we proved that IRAK2 was another target of miR-146a, which also participated in VSV-induced type I IFN production. Furthermore, IRAK1 and IRAK2 participated in VSV-induced type I IFN production by associating with Fas-associated death domain protein, an important adaptor in RIG-I signaling, in a VSV infection-inducible manner. Therefore, we demonstrate that miR-146a, up-regulated during viral infection, is a negative regulator of the RIG-I-dependent antiviral pathway by targeting TRAF6, IRAK1, and IRAK2.   *The Journal of Immunology,* 2009, 183: 2150–2158.

E
ffective recognition of viral infection and subsequent triggering of antiviral innate and adaptive immune response are essential for the survival of the host. Upon recognition of viral components, host cells are activated to produce type I IFN and proinflammatory cytokines (1–4). Type I IFN, IFN-β, and many IFN-α species play pivotal roles in antiviral immune responses. A suitable amount of type I IFN production induces cellular resistance to viral infection and apoptosis of virus-infected cells (5, 6). However, excessive production of type I IFN may promote the development of immunopathological conditions or immune disorders. Hence, type I IFN production during virus infection should be tightly controlled to initiate an appropriate immune response for eliminating the invading pathogens while avoiding immune disorders (7). Alternatively, viruses have developed several strategies to evade and subvert the immune responses for their survival in host cells. Disruption of host recognition and subsequent impairment of type I IFN production is one well-known evading strategy for viruses (8, 9). However, the underlying mechanisms for this evading strategy of viruses remain to be fully understood.

Viruses have been shown to be recognized by pattern recognition receptors, including TLRs and retinoic acid-inducible gene I (RIG-I)[4]-like helicases (RLH). RIG-I was identified as a cytoplasmic viral RNA detector (10). It contains two N-terminal caspase recruitment domains (CARD) and a C-terminal helicase domain. Upon binding to intracellular viral RNA through its helicase domain, downstream signaling cascades of the RIG-I pathway were initiated through the N-terminal CARDs (10). The CARDs associate with IFN-β promoter stimulator-1, another CARD containing molecule, which in turn activates Fas-associated death domain (FADD) and TANK binding kinase-1-IκB kinase-ε via TNFR-associated factor (TRAF) 3, resulting in the activation of NF-κB, IFN regulatory factor 3 and IFN regulatory factor 7, and then contributes to the production of type I IFN to overcome viral infection (3). It has been shown that RIG-I-deficient cells do not produce type I IFN in response to infection of vesicular stomatitis virus (VSV), suggesting that RIG-I is the main sensor of the host to recognize VSV and subsequently initiate immune response to eliminate VSV infection (11). Up to now, multiple negative regulators of RIG-I signaling, such as deubiquitinating enzyme A and nucleotide-binding domain and leucine-rich repeat X1, have been

*Institute of Immunology, Tsinghua University School of Medicine, Beijing, China; [†]National Key Laboratory of Medical Immunology and Institute of Immunology, Second Military Medical University, Shanghai, China; [‡]Institute of Immunology, Zhejiang University School of Medicine, Hangzhou, China; and [§]Department of Medical Genetics, Shanghai Jiao Tong University School of Medicine, Shanghai, China

[4] Abbreviations used in this paper: RIG-I, retinoic acid-inducible gene I; RLH, RIG-I-like helicase; miRNA, microRNA; VSV, vesicular stomatitis virus; CARD, caspase recruitment domain; FADD, Fas-associated death domain-containing protein; TRAF, TNFR-associated factor; MyD88, myeloid differentiation factor 88; UTR, untranslational region; IRAK, IL-1R-associated kinase; TCID$_{50}$, 50% tissue culture infectious dose; poly(IC), polyinosinic-polycytidylic acid; PDTC, pyrrolidinecarbodithioic acid; BMDC, bone marrow-derived dendritic cell; MOI, multiplicity of infection; TRIF, Toll-IL-1R domain-containing adaptor inducing IFN-β; q-RT-PCR, quantitative RT-PCR; MEF, mouse embryonic fibroblast.

identified to inhibit RIG-I-dependent type I IFN production, which may help host to avoid immune disorders mediated by uncontrolled or excessive production of type I IFN (12, 13). Alternatively, viruses can disrupt the RIG-I signaling pathway and thus inhibit RIG-I-mediated antiviral activities in host cells through many viral components or responsive host negative regulators (8, 14). In addition to the miRNAs encoded by viruses themselves, viral infection has been found to be able to up-regulate or down-regulate expression of miRNAs in host cells (15). However, to date, there is no report about the regulation of RIG-I signaling pathway by miRNAs during viral infection.

miRNAs, an abundant class of highly conserved small (18–25 nt long) noncoding RNAs, suppress gene expression by binding to the the 3′-untranslational region (UTR) of target mRNAs, which presents an entirely new approach to posttranscriptional regulation of gene expression. miRNAs play key roles in the regulation of diverse biological processes, such as development, infection, immune response, inflammation, and tumorigenesis (16, 17). Since the initial observation, >700 miRNAs have been identified in mammals, and the biological functions of a large part remain illusive. Various functions of miRNAs in immune responses are now emerging (18–21). Direct roles of miRNAs in innate immune response were initiated by a report that identified miR-146a as a negative feedback regulator in TLR signaling by targeting IL-1R-associated kinase (IRAK) 1 and TRAF6 (22). Further reports showed that EBV-encoded latent membrane protein 1 and proinflammatory cytokine IL-1β also induced the expression of miR-146a (23–25). miR-146a was decreased by estrogen treatment and in turn led to the augmentation of LPS-induced IFN-γ and inducible NO synthase-NO production in splenic lymphocytes, further confirming that miR-146a is a negative regulator of TLR signaling (26). Given the important roles of the RIG-I signaling pathway in innate antiviral immune response, whether and how RIG-I signaling and RIG-I-dependent type I IFN production in innate immune cells are regulated by miRNAs, including miR-146a, need to be investigated.

In the present study, we first analyzed the expression profile of miRNAs in mouse peritoneal macrophages during VSV infection. We found that several miRNAs, including miR-146a, miR-155, miR-7a, miR-574–5p, and miR-125a-5p were significantly up-regulated and that VSV infection could up-regulate miR-146a expression in macrophages through a TLR-myeloid differentiation factor 88 (MyD88)-independent but RIG-I-NF-κB-dependent manner. Then we focused on the regulation of RIG-I signaling by the inducible miR-146a and demonstrated that miR-146a feedback negatively regulated VSV infection-triggered type I IFN production by impairing RIG-I pathway through targeting TRAF6, IRAK1, and also IRAK2, which was firstly identified as another target of miR-146a and a molecule involved in RIG-I signaling. Furthermore, we found IRAK1 and IRAK2 associated with FADD, an important adaptor in RIG-I signaling, in a VSV infection-inducible manner. We for the first time demonstrate that miR-146a is a feedback negative regulator of the RIG-I signaling and RIG-I-dependent antiviral pathways.

Materials and Methods
Mice and reagents

C57BL/6 mice (6–8 wk) were obtained from Joint Ventures Sipper BK Experimental Animal. TLR3 knockout mice was obtained from The Jackson Laboratory (B6;129S1-*Tlr3*^*tm1Flv*^/J; 005217; The Jackson Laboratory). TLR4, TLR9, or MyD88 knockout mice were gifts from Prof. Shizuo Akira. RIG-I knockout mice were generated as described previously (27, 28). All animal experiments were undertaken in accordance with the National Institute of Health Guide for the Care and Use of Laboratory Animals, with the approval of the Scientific Investigation Board of Second

Military Medical University (Shanghai, China). TLR ligands peptidoglycan, polyinosinic-polycytidylic acid (poly(IC)), LPS, R837, and CpG were described previously (29, 30). VSV was a gift from Prof. Wei Pan. VSV M4, a VSV mutant containing mutations in its possible miR-146a target site, was kindly provided by Prof. Jiahuai Han (31). Pyrrolidinecarbodithoic acid (PDTC), an inhibitor of NF-κB, was purchased from Calbiochem. Mouse rIFN-β and anti-IFN-β-neutralizing Ab were obtained from PBL. Abs specific to TRAF6, IRAK1, IRAK2, FADD, and HRP-coupled secondary Abs were from Santa Cruz Biotechnology. Ab specific to phosphorylated IκBα was from Cell Signaling Technology. Ab specific to β-actin was from Sigma-Aldrich.

Cell culture and transfection

HEK293 cell line was obtained from American Type Culture Collection (ATCC) and cultured as described previously (29). 1×10^4 cells were seeded into 96-well plates and incubated overnight. JetSI-ENDO transfection reagents (Polyplus transfection) were used for the cotransfection of plasmids and RNAs according to the manufacturer's instructions. Thioglycolate-elicited mouse peritoneal macrophages were prepared and cultured as described previously (29, 30). Into each well 0.5 ml of 2×10^5 cells was seeded into 24-well plates and incubated overnight and then transfected with RNAs using INTERFERin (Polyplus transfection) according to the manufacturer's instructions. Splenocytes and bone marrow-derived dendritic cells (BMDC) were generated as described previously (32).

Paraflo miRNA microarray assay

The miRNA microarray assay was conducted by a service provider (LC Sciences). In brief, the assay was performed on 5 μg of total RNA samples from normal macrophages (labeled Cy3) and macrophages infected by VSV at a multiplicity of infection (MOI) of 10 for 48 h (labeled Cy5). The small RNAs (<200 nt) were 3′-extended with a polyadenylate tail using polyadenylate (poly(A) polymerase and then ligated to an oligonucleotide tag for later staining. Hybridization was done overnight on a μParaFlo microfluidic chip using a microcirculation pump (Atactic Technologies; Ref. 33). After hybridization, images were collected and quantified. The differentially detected signals were presented in supplemental Fig. 1A[5] ($p < 0.01$). The microarray data were submitted to the Minimum Information About a Microarray Experiment (MIAME) database with the accession number E-MEXP-2110 (http://www.ebi.ac.uk/microarray-as/ae/).

miRNA mimics and inhibitors

miR-146a mimics (dsRNA oligonucleotides) and miR-146a inhibitors (single-stranded chemically modified oligonucleotides) from GenePharma were used for the overexpression and inhibition of miR-146a activity in mouse peritoneal macrophages, respectively. Macrophages described above were transfected with RNAs at a final concentration of 10 nM. Negative control mimics or inhibitors (GenePharma) were transfected as matched controls.

RNA interference

The TRAF6-specific siRNAa were 5′-CAUUAAGGAUGAUACAUUA TT-3′ (sense) and 5′-UAAUGUAUCAUCCUUAAUGAA-3′ (antisense). The IRAK1-specific siRNAs were 5′-AGUGGUAGACAUGUAGGA GTT-3′ (sense) and 5′-CUCCUACAUGUCUACCACUTT-3′ (antisense). The IRAK2-specific siRNAs were 5′-CAGUCUAAGUAUUGCAGUA TT-3′ (sense) and 5′-UACUGCAAUACUUAGACUGGG-3′ (antisense). The MyD88-sinecific siRNAs were 5′-GACUGAUUCCUAUUAAAUA-3′ (sense) and 5′-UAUUUAAUAGGAAUCAGUC-3′ (antisense). The FADD-specific siRNAs were 5′-ACGAUCUGAUGGAGCUCAATT-3′ (sense) and 5′-UUGAGCUCCAUCAGAUCGUTT-3′ (antisense). The Toll-IL-1R domain-containing adaptor inducing IFN-β (TRIF)-specific siRNAs were from Qiagen. The scrambled control RNA sequences were 5′-UUCUCCGAACGUGUCACGUTT-3′ (sense) and 5′-ACGUGACA CGUUCGGAGAATT-3′ (antisense). siRNA duplexes were transfected into mouse peritoneal macrophages at a final concentration of 10 nM.

3′-UTR luciferase reporter assays

The IRAK2 3′-UTR luciferase reporter construct was made by amplifying the mouse IRAK2 mRNA 3′-UTR sequence by PCR and cloned into theh *Xba*I site of pGL3-promoter construct (Promega). HEK293 cells described above were cotransfected with 80 ng of luciferase reporter plasmid, 40 ng

---

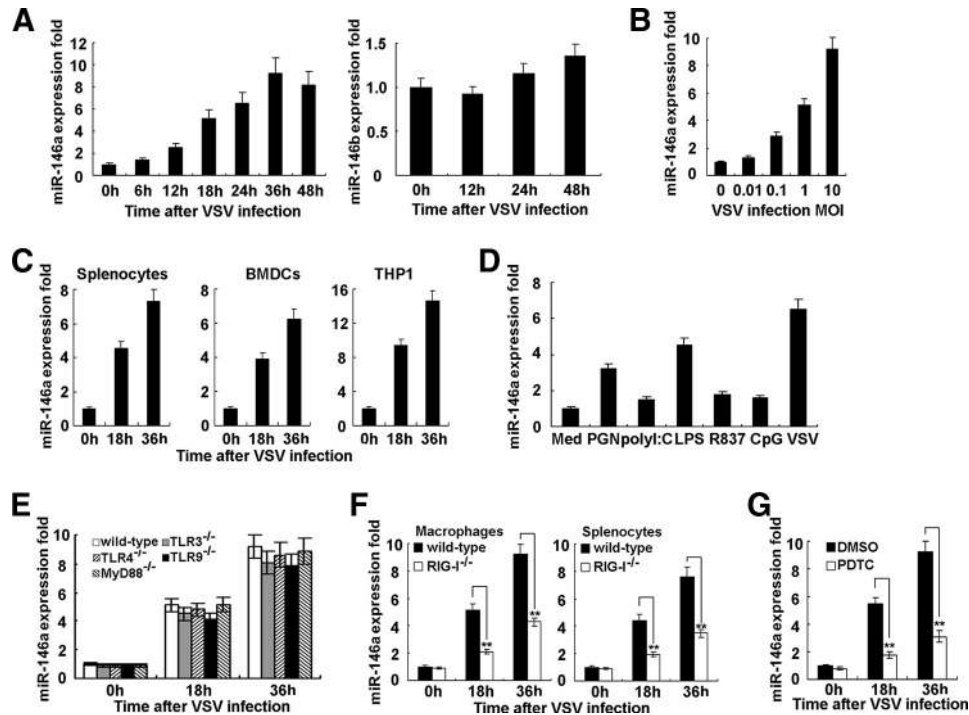[5] The online version of this article contains supplemental material.

FIGURE 1. VSV infection induces miR-146a expression in macrophages. *A*, Mouse peritoneal macrophages were infected with or without VSV at MOI 10 for indicated time. The expressions of miR-146a and miR-146b were measured by q-PCR and normalized to the expression of U6 in each sample. *B*, Mouse peritoneal macrophages were infected with or without VSV at indicated MOI for 36 h, and expression miR-146a was measured as described in *A*. *C*, Mouse splenocytes (*left*), BMDCs (*middle*), and THP-1 human monocytic cells (*right*) were infected with or without VSV at MOI 10 for the indicated time, and miR-146a expression was measured as described in *A*. *D*, Mouse peritoneal macrophages were treated with the indicated stimuli for 24 h, and miR-146a expression was measured as described in *A*. PGN, peptidoglycan; Med, medium. *E*, Peritoneal macrophages from wild-type or TLR3-, TLR4-, TLR9-, or MyD88-deficient mice were infected with or without VSV at MOI 10 for indicated time, and miR-146a expression was measured as described in *A*. *F*, Mouse peritoneal macrophages (*left*) or splenocytes (*right*) from wild-type or RIG-I-deficient mice were infected with or without VSV at MOI 10 for the indicated time, and miR-146a expression was measured as described in *A*. *G*, Mouse peritoneal macrophages were pretreated with DMSO or PDTC (100 μM) for 30 min and then infected with VSV at MOI 10 for indicated time. MiR-146a expression was measured as described in A. Data are the mean $\pm$ SD ($n = 4$) of one representative experiment. Similar results were obtained in three independent experiments. $**$, $p < 0.01$.

of pRL-TK-*Renilla*-luciferase plasmid, and the indicated RNAs (final concentration, 20 nM). After 24 h, luciferase activities were measured using the Dual-Luciferase Reporter Assay System (Promega) according to the manufacturer's instructions. Data was normalized for transfection efficiency by dividing firefly luciferase activity with that of *Renilla* luciferase.

RNA quantification

Total RNA, containing miRNA, was extracted with TRIzol reagent (Invitrogen) following the manufacturer's instructions. Real-time quantitative RT-PCR analysis was performed using the LightCycler (Roche) and SYBR RT-PCR kits (Takara). For miRNA analysis, RT primers for miR-146a and miR-146b were 5'-GTCGTATCCAGTGCAGGGTCCGAGGTAT TCGCACTGGATACGACAACCC-3' and 5'-GTCGTATCCAGTGCA GGGTCCGAGGTATTCGCACTGGATACGACAGCCT-3', respectively. Quantitative PCR (q-PCR) primers were 5'-AGCAGTGAGAACTGAATT CCAT-3' (forward) and 5'-GTGCAGGGTCCGAGGT-3' (reverse). Similarly, U6 small nuclear RNA was quantified using its reverse primer for RT reaction and its forward and reverse primers for q-PCR, which was 5'-CTCGCTTCGGCAGCACA-3' (forward) and 5'-AACGCTTCACGA ATTTGCGT-3' (reverse). The relative expression level of miRNAs was normalized to that of internal control U6 by using $2^{-\Delta\Delta C_t}$ cycle threshold method (34). For mouse β-actin, IFN-β, and IFN-4α mRNA analysis, the primers were described previously (29, 30); for mouse IRAK2, the primers were: 5'-GGAGTGAAGCAGATGTCGTCCAAGC-3' (forward) and 5'-GCATCTGAGGCAGAGCTGCATCTCT-3' (reverse); for VSV Indiana serotype, the primers were: 5'-ACGGCGTACTTCCAGATGG-3' (forward) and 5'-CTCGGTTCAAGATCCAGGT-3' (reverse). Data were normalized by the level of β-actin expression in each sample as described above.

ELISA

Into each well of 24-well plates, 0.5 ml of 2×10^5 cells was seeded, incubated overnight, and then transfected as described above. After 48 h,

the cells were infected with VSV for indicated time periods. The concentrations of IFN-β in culture supernatants were measured with an ELISA kit (PBL). ELISA kits for IL-8 and RANTES were from R&D Systems. ELISA kits for IL-1β, IL-6, and TNF-α were from BioSource.

Immunoblot and immunoprecipitation

Cells were lysed using M-PER protein extraction reagent (Pierce) supplemented with protease inhibitor mixture (Calbiochem). Protein concentrations of the extracts were measured with a BCA assay (Pierce) and equalized with the extraction reagent. Equal amounts of the extracts were used for immunoprecipitation or loaded and subjected to SDS-PAGE, transferred onto nitrocellulose membranes, and then blotted as described previously (29, 30).

Flow cytometry

HEK293 cells were cotransfected with GFP-empty plasmids or GFP-IRAK2 3'-UTR plasmids, together with control mimics or miR-146a mimics. At 24 h posttransfection, cells were subjected to flow cytometric analysis on a FACSCalibur, and data were analyzed with CellQuest software (both from BD Biosciences). The mean fluorescence intensity and positive percentage rate of green-fluorescing cells were determined.

VSV yield qualification

Macrophages were transfected and infected by VSV as indicated. 0.1 ml of the cultural supernatants were serially diluted on the monolayer of BHK21 cells, which were obtained from ATCC, and 1×10^4 cells were seeded into 96-well plates 1 day before measurement. The 50% tissue culture infectious dose (TCID$_{50}$) was measured after 3 days. Viral RNA in the supernatant was extracted using the Body Fluid Viral DNA/RNA Miniprep Kit (Axygen) and VSV RNA replicates were qualified as described above.
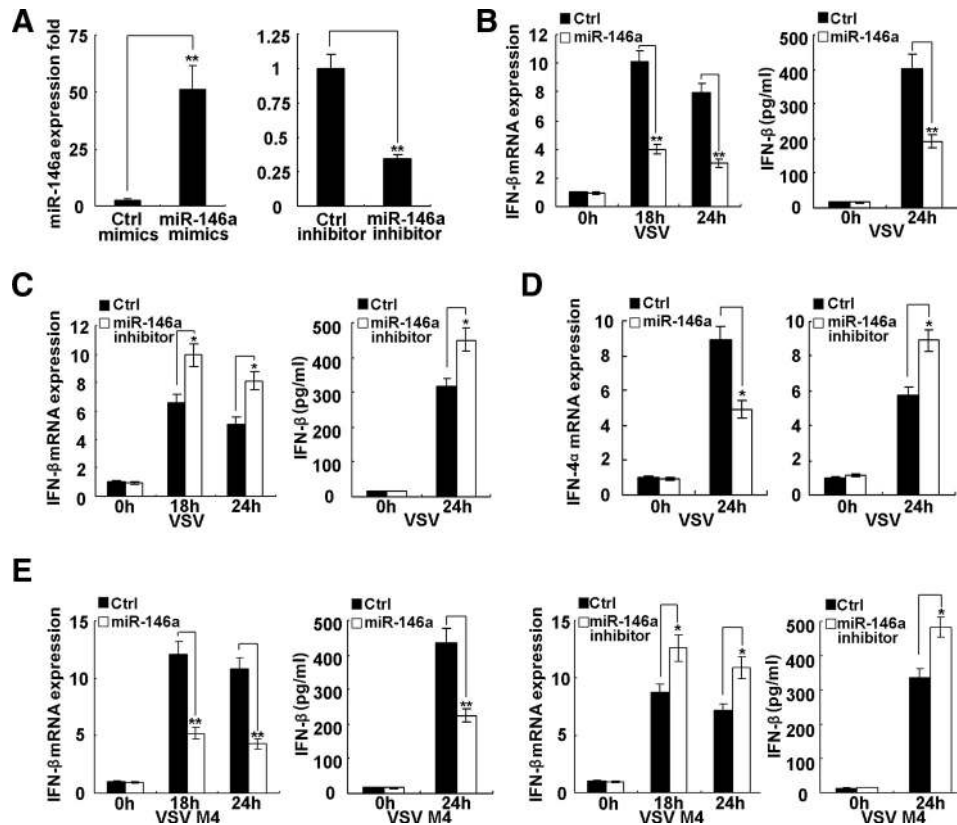
FIGURE 2. miR-146a negatively regulates VSV-triggered type I IFN production. *A*, 0.5 ml of 2×10^5 mouse peritoneal macrophages were transfected with ctrl mimics or miR-146a mimics (*left*), control (ctrl) inhibitor or miR-146a inhibitor (*right*) as indicated at a final concentration of 10 nM. After 48 h, miR-146a expression was measured as described in Fig. 1*A*. *B* and *C*, Macrophages described in *A* were transfected with control mimics or miR-146a mimics (*B*), control inhibitor or miR-146a inhibitor (*C*) as indicated. After 48 h, cells were infected by VSV at MOI 10 for indicated time. IFN-β mRNA expression (*left*) was measured by q-PCR and normalized to the expression of β-actin in each sample. IFN-β in supernatants (right) was measured by ELISA. *D*, Macrophages were transfected and infected as described in *B* and *C*, and IFN-4α mRNA expression was measured as described in *B* and *C*. *E*, Macrophages were transfected as described in *B* and *C* and then infected by VSV M4 at MOI 10 for indicated time. IFN-β was measured as described in *B* and *C*. Data are the mean ± SD ($n = 4$) of one representative experiment. Similar results were obtained in three independent experiments. ∗∗, $p <$ 0.01; ∗, $p < 0.05$.

Statistical analysis

Statistical significance was determined by Student's *t* test, with *p* values of <0.05 considered to be statistically significant.

Results

VSV infection up-regulates miR-146a expression in macrophages through TLR-MyD88-independent but RIG-I/NF-κB-dependent pathways

To investigate whether and what miRNAs expression might be regulated by VSV challenge, we analyzed the miRNA expression profile of mouse primary peritoneal macrophages infected with VSV by using an array-based miRNA profiling. After the infection of VSV at MOI 10 for 48 h, the array revealed that many miRNAs were up-regulated in macrophages, and the top five of these VSV infection-up-regulated miRNAs were miR-146a, miR-155, miR-7a, miR-574-5p, and miR-125a-5p (supplemental Fig. 1*A*). This result was further confirmed by qRT-PCR analysis for the up-regulation of miRNAs described before in VSV-challenged macrophages (supplemental Fig. 1*B*). Considering that miR-146a, identified to be a feedback negative regulator of TLR signaling (22), is significantly up-regulated by VSV infection, but there is no report to date about the regulation of RIG-I signaling by miR-146a, we focused on the roles and the underlying mechanisms of miRNA-146a in the RIG-I-signaling and RIG-I-dependent antiviral innate immune responses.

Induction of mature miR-146a following VSV challenge, as detected by qRT-PCR in Fig. 1*A*, indicated that miR-146a was a VSV infection-responsive gene in macrophages. Its induction increased to the peak at ~36 h after VSV challenge. However, mature miR-146b, a homolog of miR-146a, was not induced in macrophages after VSV infection (Fig. 1*A*). Furthermore, VSV induced miR-146a expression in a dose-dependent manner (Fig. 1*B*). In addition to its up-regulation in macrophages, miR-146a expression was also up-regulated by VSV infection in mouse splenocytes, BMDCs, and THP-1 human monocytic cells (Fig. 1*C*). Similar to a previous report (22), expression of miR-146a could be induced by ligands of TLR2 and TLR4 in mouse peritoneal macrophages, but we found that ligands of TLR3, TLR7, and TLR9 could not up-regulate miR-146a expression (Fig. 1*D*).

Peritoneal macrophages from TLR3, TLR4, TLR9, or MyD88-deficient mice were prepared and infected with VSV, and we found that induction of miR-146a expression following VSV infection was comparable with that in normal macrophages (Fig. 1*E*), thus excluding the possibility that activation of TLR signals might contribute to VSV-induced miR-146a expression in macrophages. However, induction of miR-146a by VSV challenge was impaired in RIG-I-deficient macrophages and splenocytes (Fig. 1*F*), suggesting that VSV-induced miR-146a expression was dependent on RIG-I signaling. As control, LPS-induced miR-146a expression was impaired by TLR4 or MyD88 deficiency, but not significantly

influenced by RIG-I deficiency (supplemental Fig. 2). Because induction of miR-146a was shown to be NF-κB-dependent (22), we went further to investigate the effect of NF-κB inhibitor on VSV-induced miR-146a expression in macrophages. As shown in Fig. 1G, inhibition of NF-κB by PDTC, a chemically synthesized inhibitor of NF-κB, impaired VSV-induced miR-146a expression. Taken together, VSV infection can induce miR-146a expression through RIG-I/NF-κB pathways but not TLR-MyD88 pathways.

miR-146a negatively regulates VSV-triggered type I IFN production in macrophages

To further identify whether VSV-induced miR-146a expression could affect VSV-triggered response in macrophages, we investigated the role of miR-146a in type I IFN production after VSV challenge. As shown in Fig. 2A, transfection of miR-146a mimics increased miR-146a expression in macrophages, whereas miR-146a inhibitor decreased its expression level. miR-146a overexpression inhibited VSV-triggered IFN-β production at both the mRNA and protein level (Fig. 2B), whereas inhibition of miR-146a promoted VSV-triggered IFN-β production (Fig. 2C). Negative regulation of VSV-triggered IFN-4α mRNA production by miR-146a was also observed, which was similar to negative regulation of IFN-β by miR-146a (Fig. 2D). Previous report showed that VSV sequence contained a possible miR-146a target site and that miR-146a had a slight effect on VSV replication (31). To exclude the possibility that the inhibition of miR-146a on type I IFN production was due to its direct effect on VSV replication, VSV M4, a mutant containing mutations in its possible miR-146a target site (31), was used in the investigation of miR-146a in regulating type I IFN production. VSV M4-induced type I IFN production was regulated by miR-146a in the same manner, as compared with type I IFN production induced by wild-type VSV (Fig. 2E). Taken together, these results demonstrate that miR-146a negatively regulates VSV-triggered type I IFN production in macrophages.

We went further to investigate the effect of miR-146a on VSV-induced production of proinflammatory cytokines and chemokines. Similar to type I IFN, miR-146a negatively regulated VSV-induced production of proinflammatory cytokines IL-1β, IL-6, and TNF-α, and chemokines IL-8 and RANTES in mouse primary peritoneal macrophages (supplemental Fig 3, A and B). Moreover, miR-146a down-regulated the phosphorylation of IκBα induced by VSV infection in macrophages, indicating that NF-κB activity is also negatively regulated by miR-146a (supplemental Fig. 3C). These results suggest that miR-146a extensively down-regulates VSV infection-induced responses in macrophages.

VSV infection-inducible miR-146a promotes VSV replication through impairment of type I IFN production

To further investigate the biological significance of the up-regulated miR-146a expression and the subsequent impairment of VSV-triggered type I IFN production, we went further to investigate the effects of inhibition of miR-146a-inducible expression on VSV replication and the role of IFN-β involved in the effect. To minimize the interaction of host miRNAs on VSV replication (31), VSV M4 was used to determine VSV replication in macrophages with or without inhibition of miR-146a-inducible expression. By measuring VSV TCID$_{50}$ in the cultural supernatants of the infected macrophages, we found that inhibition of miR-146a-inducible expression, just like addition of recombinant IFN-β, could inhibit VSV replication, whereas anti-IFN-β-neutralizing Ab could reverse the suppression of VSV replication by the miR-146a inhibitor, indicating that the impairment of IFN-β production by miR-146a may help VSV replication (Fig. 3A). Furthermore, inhibition
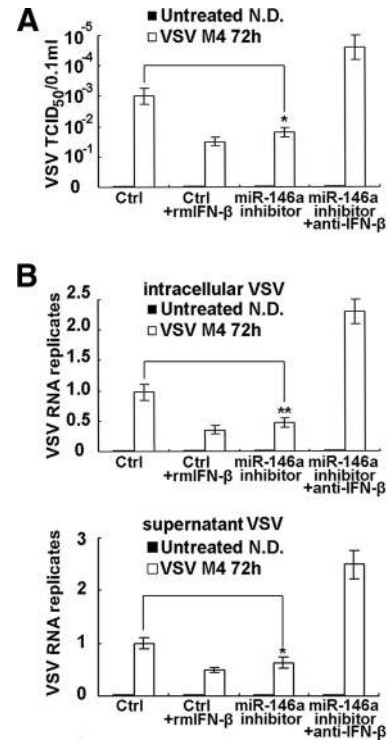

FIGURE 3. Inhibition of miR-146a-inducible expression in macrophages suppresses VSV replication. *A*, Mouse peritoneal macrophages were transfected with control (ctrl) inhibitor or miR-146a inhibitor as in Fig. 2A. After transfection for 48 h, cells were infected by VSV M4 at MOI 10 for 1 h and washed, then fresh medium or fresh medium containing recombinant mouse IFN-β (100 U/ml) or anti-IFN-β-neutralizing Ab (100 neutralizing units/ml) were added as indicated. After 72 h, virus in supernatants were serially diluted on the monolayer of BHK21 cells and TCID$_{50}$ was measured (N.D., not detected). *B*, Mouse peritoneal macrophages were treated as described in *A*, and intracellular (*left*) VSV RNA replicates were qualified using qRT-PCR and normalized to the expression of β-actin in each sample. Supernatant (*right*) VSV replicates were measured by extracting RNA from equal volume of cultural supernatants and using qRT-PCR for qualification. Data are the mean $\pm$ SD ($n = 4$) of one representative experiment. Similar results were obtained in three independent experiments. **, $p < 0.01$; *, $p < 0.05$.

of miR-146a-inducible expression could suppress intracellular and supernatant VSV RNA replicates in macrophages (Fig. 3B). These results demonstrate that VSV infection-induced up-regulation of miR-146a can in turn promote VSV replication in macrophages through impairment of type I IFN production.

miR-146a targets TRAF6, IRAK1, and IRAK2

Next, we examined the possible targets of miR-146a, which might modulate VSV-triggered type I IFN production. As predicted, the expression of TRAF6 and IRAK1, two known miR-146a targets, were decreased in macrophages transfected with miR-146a, as compared with that of control cells; and inhibition of miR-146a enhanced the expression of TRAF6 and IRAK-1 (Fig. 4A).

By prediction of new targets of miR-146a via TargetScan (http://www.targetscan.org), we found that mouse IRAK2 had three putative miR-146a target sites (Fig. 4B). To certify the possibility that IRAK2 was regulated posttranscriptionally by miR-146a, we constructed reporter plasmids by cloning $\approx$1 kb of the 3′-UTR from mouse IRAK2 to the 3′-UTR region of firefly luciferase gene or GFP gene. By cotransfection of the reporter plasmids and internal control pRL-TK-*Renilla*-luciferase plasmids with miR-146a mimics or inhibitors in HEK293 cells, we observed that
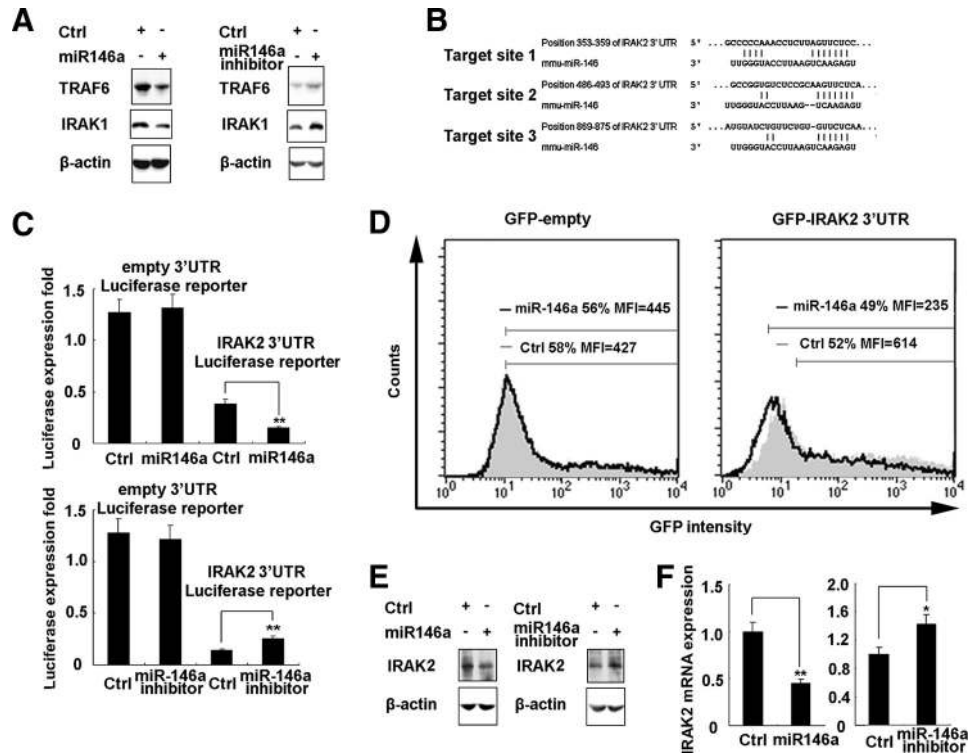
FIGURE 4. miR-146a targets mouse TRAF6, IRAK1, and IRAK2. *A*, Mouse peritoneal macrophages (1×10^6) were transfected as described in Fig. 2*A*. After 48 h, TRAF6, IRAK1, and β-actin were detected by immunoblot. *B*, Mouse IRAK2 might be molecular target of miR-146a. Shown is a sequence alignment of miR-146a and its target sites in 3′-UTR of IRAK2, which was downloaded from TargetScan (http://www.targetscan.org). *C*, HEK293 cells (1×10^4) were cotransfected with 80 ng of pGL3-promoter firefly luciferase reporter plasmids or pGL3-IRAK2 3′-UTR firefly luciferase reporter plasmids, 40 ng of pTK-*Renilla*-luciferase plasmids, together with control (ctrl) mimics or miR-146a mimics, control inhibitor, or miR-146a inhibitor (final concentration: 20 nM) as indicated. After 24 h, firefly luciferase activity was measured and normalized by *Renilla* luciferase activity. *D*, HEK293 cells (1×10^5) were cotransfected with 400 ng of GFP expression plasmids or GFP-IRAK2–3′-UTR plasmids, together with control mimics or miR-146a mimics (final concentration, 20 nM) as indicated. After 24 h, GFP expression was analyzed by FACS and the mean fluorescence intensity (MFI) of GFP was determined. *E* and *F*, Mouse peritoneal macrophages (1×10^6) were transfected as described in Fig. 2*A*. After 48 h, IRAK2 and β-actin were detected by immunoblot (*E*), and IRAK2 mRNA was measured as described in Fig. 2, *B* and *C*. Data are the mean ± SD ($n = 4$) of one representative experiment. Similar results were obtained in at least three independent experiments. **, $p < 0.01$; *, $p < 0.05$.

miR-146a mimics markedly decreased the luciferase level whereas miR-146a inhibitors increased its level (Fig. 4*C*). MiR-146a also down-regulated GFP gene expression when the 3′-UTR of IRAK2 was cloned into the 3′-UTR region of GFP (Fig. 4*D*). Furthermore, transfection of miR-146a mimics decreased IRAK2 expression in macrophages at both the protein and mRNA levels, whereas miR-146a inhibitors increased IRAK2 expression (Fig. 4, *E* and *F*), suggesting that IRAK2 expression could be inhibited by miR-146a via both translational inhibition and mRNA degradation. Together, the results show that expression of endogenous mouse IRAK2 is targeted and regulated by miR-146a, and mouse IRAK2 is a new target of miR-146a.

Knockdown of miR-146a targets inhibits VSV-triggered type I IFN production

To further investigate the mechanisms by which VSV-triggered type I IFN production was regulated by miR-146a, we examined the effects of knockdown of miR-146a targets on VSV-triggered type I IFN production. siRNA specific to mouse TRAF6, IRAK1, or IRAK2 significantly inhibited the expression of TRAF6, IRAK1, or IRAK2 respectively (Fig. 5*A*). In mouse peritoneal macrophages, respective knockdown of TRAF6, IRAK1, or IRAK2 markedly reduced VSV-triggered type I IFN production (Fig. 5, *B–D*). These data suggest that negative regulation of VSV-triggered type I IFN production by miR-146a could be mediated by knockdown of its targets TRAF6, IRAK1, and IRAK2. Poly(IC) is believed to be

sensed by another RLH melanoma differentiation-associated gene-5 (*MDA-5*; Ref. 35). Moreover, knockdown of TRAF6, IRAK1, or IRAK2 also inhibited transfection of poly(IC)-induced IFN-β production in TLR3-deficient macrophages, and knockdown of MyD88 or TRIF had little effect on VSV-induced IFN-β production (Fig. 5*E* and supplemental Fig. 4). These results further confirmed that TRAF6, IRAK1, and IRAK2 participate in RLH-mediated type I IFN production independent of TLRs.

IRAK1 and IRAK2 participate in VSV-induced type I IFN production by associating with FADD

A recent report showed that VSV-triggered type I IFN production was severely impaired in TRAF6 knockout mouse embryonic fibroblasts (MEF; Ref. 36), the mechanism of which might be the lack of interaction between TRAF6 and IFN-β promoter stimulator-1 (37). In mouse peritoneal macrophages, TRAF6 might participate in RIG-I signaling by a similar mechanism. To elucidate the mechanism by which IRAK1 and IRAK2 participate in VSV-induced type I IFN production, we pulled down IRAK1 or IRAK2 from macrophages after VSV challenge. In the precipitates, FADD, an important adapter in RIG-I-dependent type I IFN production (38, 39), was detected in a VSV-induced manner (Fig. 6*A*), suggesting that IRAK1 and IRAK2 could associate with FADD to participate in VSV-induced type I IFN production. Accordingly, precipitation with FADD Ab also pulled down IRAK1 and IRAK2 (Fig. 6*B*), which further confirmed their association. Furthermore,
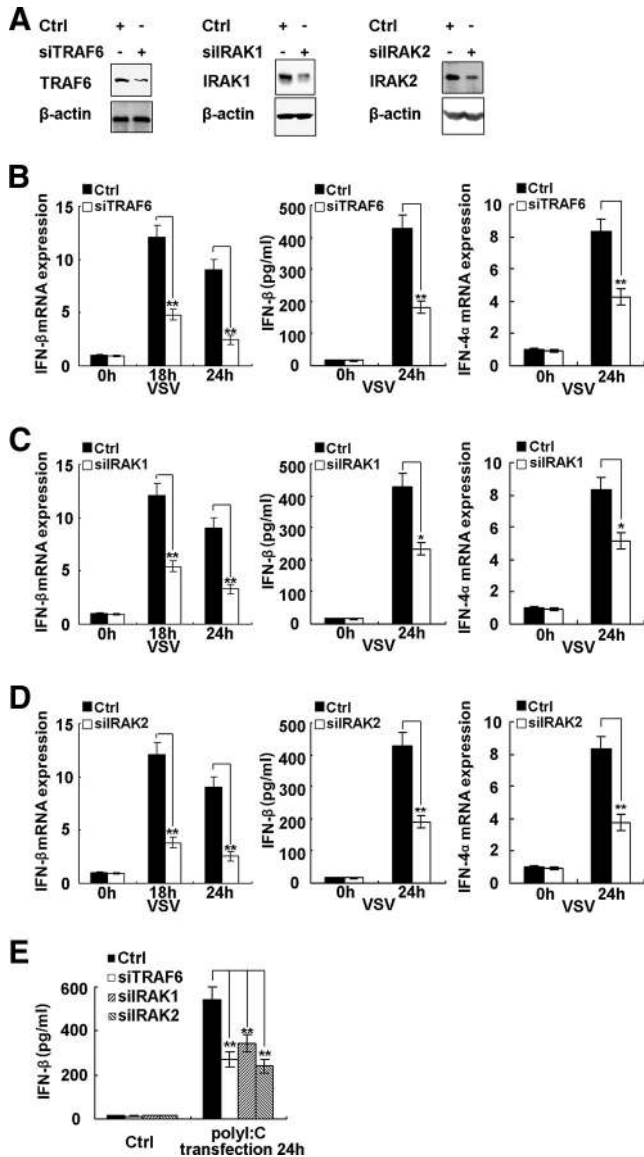
FIGURE 5. Knockdown of miR-146a targets inhibits VSV-triggered type I IFN production in macrophages. *A*, Mouse peritoneal macrophages (1×10^6) were transfected with ctrl RNA, TRAF6 siRNA (*left*), IRAK1 siRNA (*middle*), or IRAK2 siRNA (*right*), respectively, as indicated at a final concentration of 10 nM. After 48 h, TRAF6, IRAK1, IRAK2, and β-actin were detected by immunoblot. *B–D*, 0.5 ml of 2×10^5 mouse peritoneal macrophages were transfected with control (ctrl) RNA, TRAF6 siRNA (*B*), IRAK1 siRNA (*C*), or IRAK2 siRNA (*D*), respectively, as indicated at a final concentration of 10 nM. After 48 h, cells were infected by VSV at MOI 10 for indicated time. IFN-β and IFN-4α were measured as described in Fig. 2, *B–D*. *E*, 0.5 ml of 2×10^5 TLR3-deficient mouse peritoneal macrophages were transfected with control RNA, TRAF6 siRNA, IRAK1 siRNA, or IRAK2 siRNA, respectively, as indicated at a final concentration of 10 nM. After 48 h, the cells were transfected with 10 μg poly(IC) using INTERFERin according to the manufacturer's instructions for 24 h. IFN-β in supernatants was measured by ELISA. Data are the mean $\pm$ SD ($n = 4$) of one representative experiment. Similar results were obtained in at least three independent experiments. **, $p < 0.01$; *, $p < 0.05$.

in FADD knockdown macrophages, knockdown of IRAK1 or -2 had little effect on VSV-induced IFN-β production (supplemental Fig. 5). These results suggest that VSV may induce association of IRAK1, IRAK2, and FADD in macrophages and that this complex might be indispensable for type I IFN production in virus-infected macrophages.
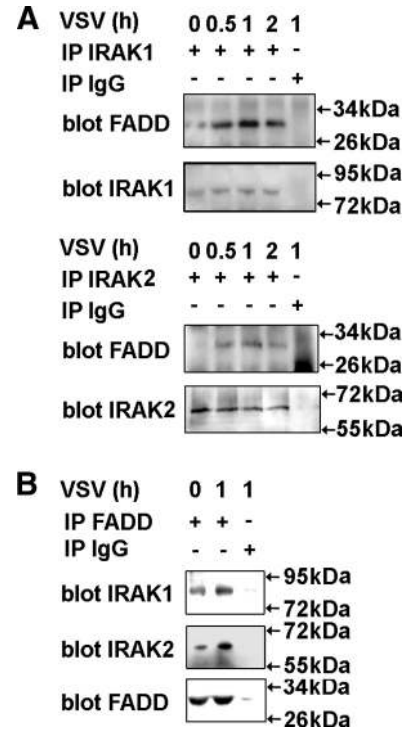

FIGURE 6. IRAK1 and IRAK2 participate in VSV-induced type I IFN production by associating with FADD. Mouse peritoneal macrophages were infected with VSV at MOI 100 for indicated time. Equal amount of cell lysates were immunoprecipitated (IP) with IRAK1, IRAK2 (*A*), FADD (*B*), or control IgG (*A* and *B*) Ab, respectively, and then immunoblotted (blot) with IRAK1, IRAK2, or FADD Ab. Data are shown of one representative experiment. Similar results were obtained in three independent experiments.

Discussion

Host defense against viral invasion requires induction of appropriate innate immune responses, but acute or chronic inflammatory disorders could be caused by excessive induction of antiviral immune response. Hence, various layers of negative regulators are used by immune cells to avoid excessive inflammation or uncontrolled immune response when encountering viral invasion. In other side, these negative regulators may also be used by viruses for their evading and subverting of the immune responses, which helps their survival in host cells. RIG-I signaling pathway plays pivotal roles in virus recognition and initiation of antiviral immune response in immune cells. Although some negative regulatory mechanisms for RIG-I-dependent antiviral immune response have been reported (40), the detailed mechanisms and the new negative regulators must be further identified. Here, we report a novel feedback negative regulator in RIG-I signaling at the level of miRNAs. First, we found that VSV infection could induce up-regulation of miR-146a expression in macrophages through TLR-MyD88-independent but RIG-I-NF-κB-dependent pathways. Second, we have proved that miR-146a negatively regulates VSV-triggered type I IFN production and that the inducible miR-146a expression could promote VSV replication by suppressing type I IFN production, thus proposing a new mechanism for the evasion of innate immune control by virus. Third, we have demonstrated that mouse TRAF6, IRAK1, and IRAK2 are miR-146a targets. Fourth, inhibition of miR-146a targets could suppress RIG-I-dependent type I IFN production, and IRAK1 and IRAK2 participate in VSV-induced type I IFN production by associating with FADD. Therefore, we present a new model that VSV infection is first

sensed by RIG-I and in turn RIG-I initiates type I IFN production against VSV infection; however, at the same time, VSV infection can also up-regulate the expression of miR-146a which in turn inhibits innate antiviral immune response by impairing RIG-I signaling and RIG-I-triggered type I IFN production. Induction of miR-146a expression may be a new strategy of virus for their survival by escaping the antiviral immune response of host.

For the involvement of TRAF6, a target of miR-146a, in RIG-I signaling, a previous report presented that normal IFN-β production was induced in TRAF6-deficient MEFs infected by Sendai virus, an RNA virus of the paramyxoviridae family that was sensed mainly through RIG-I (41). In contrast, our work showed that knockdown of TRAF6 in mouse macrophages decreased the type I IFN production in response to VSV challenge. Our results were consistent with a recent report that the RIG-I antiviral pathway was impaired in TRAF6-deficient MEFs and conventional dendritic cells (36). These discrepancies may be due to different viruses used in these studies. For the involvement of IRAK1 in RIG-I signaling, we previously reported that RIG-I-induced expression of the IFN-β reporter gene was more significant in IRAK1-deficient HEK293 cells than that in wild-type HEK293 cells (30), which might be in conflict to the function of IRAK1 in the present study. The discrepancy may be the different roles of IRAK1 in mouse macrophages and in HEK293 cells. For IRAK2, a previous report demonstrated its pivotal roles in TLR signaling in vivo by using IRAK2-deficient mice (42). Here, we found that IRAK2 also participated in VSV-induced type I IFN production by associating with FADD.

Extensive investigation of TLR signaling has demonstrated that ligation of TLR induces the activation of IRAK1 and IRAK2, both of which contain TRAF6-binding motif and in turn associate with TRAF6 to relay signals (42–44). However, following VSV infection, TRAF6 was not detected in the precipitates pulled down by IRAK1 or IRAK2 in our experiments (data not shown), suggesting that IRAK1/2-TRAF6 association is not induced in the activation of RIG-I signals. A previous report showed that FADD interacts with IRAK1 following LPS stimulation and then is shuttled to MyD88 to attenuate LPS-induced response by interference with IRAK1-MyD88 interaction (45). Here, we demonstrated that VSV infection led to association of IRAK1 and IRAK2 with FADD to relay signals, the mechanism of which might also be the death domain-death domain interaction. The interaction of IRAK1/2 and FADD may be indispensable for VSV-induced type I IFN production, which is opposite to the role of negative regulation of this complex in TLR signals.

miRNAs have been thought to target multiple mRNAs, named targetome, to regulate gene expression. A single miRNA might tune protein synthesis from thousands of genes by direct or indirect effects (46). In the present study, mouse IRAK2 was proved to be a novel target of miR-146a and contribute to the feedback negative regulatory function of miR-146a in RIG-I signaling. It is probable that we are far from unveiling the last target of miR-146a, and some of the potential targets might also regulate the RIG-I antiviral response. This presumption may raise interesting future work to reveal the entire functions of miR-146a in innate immune response.

Acknowledgments

Disclosures

References

1. Akira, S., S. Uematsu, and O. Takeuchi. 2006. Pathogen recognition and innate immunity. *Cell* 124: 783–801.
2. Beutler, B., C. Eidenschenk, K. Crozat, J. L. Imler, O. Takeuchi, J. A. Hoffmann, and S. Akira. 2007. Genetic analysis of resistance to viral infection. *Nat. Rev. Immunol.* 7: 753–766.
3. Takeuchi, O., and S. Akira. 2008. MDA5/RIG-I and virus recognition. *Curr. Opin. Immunol.* 20: 17–22.
4. Vaidya, S. A., and G. Cheng. 2003. Toll-like receptors and innate antiviral responses. *Curr. Opin. Immunol.* 15: 402–407.
5. Taniguchi, T., and A. Takaoka. 2001. A weak signal for strong responses: interferon-α/β revisited. *Nat. Rev. Mol. Cell Biol.* 2: 378–386.
6. Honda, K., A. Takaoka, and T. Taniguchi. 2006. Type I interferon gene induction by the interferon regulatory factor family of transcription factors. *Immunity* 25: 349–360.
7. Liew, F. Y., D. Xu, E. K. Brint, and L. A. O'Neill. 2005. Negative regulation of Toll-like receptor mediated immune responses. *Nat. Rev. Immunol.* 5: 446–458.
8. Hengel, H., U. H. Koszinowski, and K. K. Conzelmann. 2005. Viruses know it all: new insights into IFN networks. *Trends Immunol.* 26: 396–401.
9. Iannello, A., O. Debbeche, E. Martin, L. H. Attalah, S. Samarani, and A. Ahmad. 2006. Viral strategies for evading antiviral cellular immune responses of the host. *J. Leukocyte Biol.* 79: 16–35.
10. Yoneyama, M., M. Kikuchi, T. Natsukawa, N. Shinobu, T. Imaizumi, M. Miyagishi, K. Taira, S. Akira, and T. Fujita. 2004. The RNA helicase RIG-I has an essential function in double-stranded RNA-induced innate antiviral responses. *Nat. Immunol.* 5: 730–737.
11. Kato, H., O. Takeuchi, S. Sato, M. Yoneyama, M. Yamamoto, K. Matsui, S. Uematsu, A. Jung, T. Kawai, K.J. Ishii, et al. 2006. Differential roles of MDA5 and RIG-I helicases in the recognition of RNA viruses. *Nature* 441: 101–105.
12. Kayagaki, N., Q. Phung, S. Chan, R. Chaudhari, C. Quan, K.M. O'Rourke, M. Eby, E. Pietras, G. Cheng, J.F. Bazan, et al. 2007. DUBA: a deubiquitinase that regulates type I interferon production. *Science* 318: 1628–1632.
13. Moore, C. B., D. T. BergstralhT, J. A. Duncan, Y. Lei, T. E. Morrison, A. G. Zimmermann, M. A. Accavitti-Loper, V. J. Madden, L. Sun, Z. Ye, et al. 2008. NLRX1 is a regulator of mitochondrial antiviral immunity. *Nature* 451: 573–577.
14. Bowie, A. G., and L. Unterholzner. 2008. Viral evasion and subversion of pattern-recognition receptor signalling. *Nat. Rev. Immunol.* 8: 911–922.
15. Gottwein, E., and B. R. Cullen. 2008. Viral and cellular microRNAs as determinants of viral pathogenesis and immunity. *Cell Host Microbe* 3: 375–387.
16. Bartel, D. P. 2004. MicroRNAs: genomics, biogenesis, mechanism, and function. *Cell* 116: 281–297.
17. Bushati, N., and S. M. Cohen. 2007. MicroRNA functions. *Annu. Rev. Cell Dev. Biol.* 23: 175–205.
18. Taganov, K. D., M. P. Boldin, and D. Baltimore. 2007. MicroRNAs and immunity: tiny players in a big field. *Immunity* 26: 133–137.
19. Baltimore, D., M. P. Boldin, R. M. O'Connell, D. S. Rao, and K. D. Taganov. 2008. MicroRNAs: new regulators of immune cell development and function. *Nat. Immunol.* 9: 839–845.
20. Lodish, H. F., B. Zhou, G. Liu, and C. Chen. 2008. Micromanagement of the immune system by microRNAs. *Nat. Rev. Immunol.* 8: 120–130.
21. Xiao, C., and K. Rajewsky. 2009. MicroRNA control in the immune system: basic principles. *Cell* 136: 26–36.
22. Taganov, K. D., M. P. Boldin, K. J. Chang, and D. Baltimore. 2006. NF-κB-dependent induction of microRNA miR-146, an inhibitor targeted to signaling proteins of innate immune responses. *Proc. Natl. Acad. Sci. USA* 103: 12481–12486.
23. Cameron, J. E., Q. Yin, C. Fewell, M. Lacey, J. McBride, X. Wang, Z. Lin, B. C. Schaefer, and E. K. Flemington. 2008. Epstein-Barr virus latent membrane protein 1 induces cellular microRNA miR-146a, a modulator of lymphocyte signaling pathways. *J. Virol.* 82: 1946–1958.
24. Motsch, N., T. Pfuhl, J. Mrazek, S. Barth, and F. A. Grässer. 2007. Epstein-Barr virus-encoded latent membrane protein 1 (LMP1) induces the expression of the cellular microRNA miR-146a. *RNA Biol.* 4: 131–137.
25. Perry, M. M., S. A. Moschos, A. E. Williams, N. J. Shepherd, H. M. Larner-Svensson, and M. A. Lindsay. 2008. Rapid changes in microRNA-146a expression negatively regulate the IL-1β-induced inflammatory response in human lung alveolar epithelial cells. *J. Immunol.* 180: 5689–5698.
26. Dai, R., R. A. Phillips, Y. Zhang, D. Khan, O. Crasta, and S. A. Ahmed. 2008. Suppression of LPS-induced Interferon-γ and nitric oxide in splenic lymphocytes by select estrogen-regulated microRNAs: a novel mechanism of immune modulation. *Blood* 112: 4591–4597.
27. Wang, Y., H. Zhang, Y. Sun, Z. Liu, L. Wang, S. Lu, H. Kong, Q. Liu, X. Li, Z. Lu, et al. 2007. Rig-I$^{-/-}$ mice develop colitis associated with downregulation of Gαi2. *Cell Res.* 17: 858–868.
28. Zhang, N., S. Shen, L. Jiang, W. Zhang, H. Zhang, Y. Sun, X. Li, Q. Huang, B. Ge, S. Chen, et al. 2008. RIG-I plays a critical role in negatively regulating granulocytic proliferation. *Proc. Natl. Acad. Sci. USA* 105: 10553–10558.

29. Liu, X., M. Yao, N. Li, C. Wang, Y. Zheng, and X. Cao. 2008. CaMKII promotes TLR-triggered proinflammatory cytokine and type I interferon production by directly binding and activating TAK1 and IRF3 in macrophages. *Blood* 112: 4961–4970.
30. An, H., J. Hou, J. Zhou, W. Zhao, H. Xu, Y. Zheng, Y. Yu, S. Liu, and X. Cao. 2008. Phosphatase SHP-1 promotes TLR- and RIG-I-activated production of type I interferon by inhibiting the kinase IRAK1. *Nat. Immunol.* 9: 542–550.
31. Otsuka, M., Q. Jing, P. Georgel, L. New, J. Chen, J. Mols, Y.J. Kang, Z. Jiang, X. Du, R. Cook, et al. 2007. Hypersusceptibility to vesicular stomatitis virus infection in Dicer1-deficient mice is due to impaired miR24 and miR93 expression. *Immunity* 27: 123–134.
32. Zhang, M., H. Tang, Z. Guo, H. An, X. Zhu, W. Song, J. Guo, X. Huang, T. Chen, J. Wang, and X. Cao. 2004. Splenic stroma drives mature dendritic cells to differentiate into regulatory dendritic cells. *Nat. Immunol.* 5: 1124–1133.
33. Gao, X., E. Gulari, and X. Zhou. 2004. In situ synthesis of oligonucleotide microarrays. *Biopolymers* 73: 579–596.
34. Livak, K. J., and T. D. Schmittgen. 2001. Analysis of relative gene expression data using real-time quantitative PCR and the $2^{-\Delta\Delta C_t}$ method. *Methods* 25: 402–408.
35. Gitlin, L., W Barchet, S. Gilfillan, M. Cella, B. Beutler, R.A. Flavell, M. S. Diamond, and M. Colonna. 2006. Essential role of *mda-5* in type I IFN responses to polyriboinosinic:polyribocytidylic acid and encephalomyocarditis picornavirus. *Proc. Natl. Acad. Sci. USA* 103: 8459–8464.
36. Yoshida, R., G. Takaesu, H. Yoshida, F. Okamoto, T. Yoshioka, Y. Choi, S. Akira, T. Kawai, A. Yoshimura, and T. Kobayashi. 2008. TNF receptor-associated factor (TRAF) 6 and MEK kinase (MEKK) 1 play a pivotal role in the retinoic-acid-inducible gene-I (*RIG-I*)-like helicase antiviral pathway. *J. Biol. Chem.* 283: 36211–36220.

37. Xu, L. G., Y. Y. Wang, K. J. Han, L. Y. Li, Z. Zhai, and H. B. Shu. 2005. VISA is an adapter protein required for virus-triggered IFN-β signaling. *Mol. Cell* 19: 727–740.
38. Balachandran, S., E. Thomas, and G. N. Barber. 2004. A FADD-dependent innate immune mechanism in mammalian cells. *Nature* 432: 401–405.
39. Balachandran, S., T. Venkataraman, P. B. Fisher, and G. N. Barber. 2007. Fas-associated death domain-containing protein-mediated antiviral innate immune signaling involves the regulation of Irf7. *J. Immunol.* 178: 2429–2439.
40. Komuro, A., D. Bamming, and C. M. Horvath. 2008. Negative regulation of cytoplasmic RNA-mediated antiviral signaling. *Cytokine* 43: 350–358.
41. Seth, R. B., L. Sun, C. K. Ea, and Z. J. Chen. 2005. Identification and characterization of MAVS, a mitochondrial antiviral signaling protein that activates NF-κB and IRF3. *Cell* 122: 669–682.
42. Kawagoe, T., S. Sato, K. Matsushita, H. Kato, K. Matsui, Y. Kumagai, T. Saitoh, T. Kawai, O. Takeuchi, and S. Akira. 2008. Sequential control of Toll-like receptor-dependent responses by IRAK1 and IRAK2. *Nat. Immunol.* 9: 684–691.
43. Akira, S., and K. Takeda. 2004. Toll-like receptor signalling. *Nat. Rev. Immunol.* 4: 499–511.
44. Keating, S. E., G. M. Maloney, E. M. Moran, and A. G. Bowie. 2007. IRAK-2 participates in multiple Toll-like receptor signaling pathways to NF-κB via activation of TRAF6 ubiquitination. *J. Biol. Chem.* 282: 33435–33443.
45. Zhande, R., S. M. Dauphinee, J. A. Thomas, M. Yamamoto, S. Akira, and A. Karsan. 2007. FADD negatively regulates lipopolysaccharide signaling by impairing interleukin-1 receptor-associated kinase 1-MyD88 interaction. *Mol. Cell Biol.* 27: 7394–7404.
46. Selbach, M., B. Schwanhäusser, N. Thierfelder, Z. Fang, R. Khanin, and N. Rajewsky. 2008. Widespread changes in protein synthesis induced by microRNAs. *Nature* 455: 58–63.